

# Modeling of non-Darcy Effects in Gas-Condensate Near-Wellbore Zones

A Departmental Note

Yulia Melnikova ( MIPT, Moscow, Russia),

Artyom Myasnikov (Schlumberger Moscow Research, Reservoir Testing)

## Abstract

A General Purpose Research code for fast/precise solution of non-Darcy multicomponent two-phase flow with phase transitions has been developed and validated against E300. Having a higher resolution and preprocessing approximation of phase diagram as options, the code provides the desired accuracy in less CPU time as conventional ones. In particular, it demonstrated good coincidence with E300 in accuracy and time consuming. A workflow that minimize the grid size and polynomial degrees requested for a specific problem solution with a desired is suggested and primarily validated. Such minimization may lead to significant decrease of CPU time which is important for heavy simulations. An attempt to apply the suggested workflow to optimize condensate recovery in gas-condensate reservoirs with high permeable zones is undertaken. The experiments with E300 simulation demonstrated the necessity of non-stationary BHP effect modeling. Dependences of the condensate mass change of at different vibration modes with and without non-Darcy effects were obtained. There are both positive and negative effects.

## Introduction

Gas-condensate field is complicated system consisting of hundreds of components. It may be difficult to evaluate the productivity of such field and, therefore, precise description of phase equilibrium is required. In the process of field exploitation the pressure may fall down below the critical point and, consequently, retrograde condensation may start. Gas under high temperature and decreasing pressure turns into liquid causing the decreasing of gas relative permeability and as result, of well productivity. Hydraulic fracturing is a common practice to improve productivity of gas-condensate wells. In this case inertial effects play significant role, as the velocity of fluid flow become high, and as a result, Darcy's law is no longer valid. It is well-known that neglecting of inertial effects may lead to overestimating of well productivity in two-three times [Mohan et al]. Naturally-fractured reservoirs deserve special attention [Belhaj et al]. Complex geometric structure of such reservoirs, containing many narrow fractures leads to increased flow rates. Also large pressure gradients may arise due to the decreasing of gas relative permeability when retrograde condensation takes place. Thus, accurate estimation of non-Darcy effects is very important to correctly evaluate the performance of field. Non-Darcy effects are especially strong in the well-bore zone, where the flow can be very different from the picture on the extent of the reservoir due to its high permeability of this zone, as well as the substantial spatial and temporal dependence. Therefore, traditional commercial simulators fields are not always suitable for modeling of such flows, especially if the purpose of the study to investigate transient effects. These effects arise, for example, in the problem of the optimization of gas condensate recovery when flow rates change unsteady. In this regard, we attempted to apply for such studies the compositional code developed at the Schlumberger Moscow Research.

Historically, the research code has been developed for making SLB streamline simulator FrontSim functionality increased, so, only 1D version was designed. In addition, the specificity of reservoir- scale simulation is a fixed computational grid. On the contrary, a researcher is free to select grid size for well-bore zone, so one may state problem concerning grid size minimization (and hence the estimated costs) by improving the scheme resolution. Although there is two-parameter higher resolution TVD scheme is implemented into research code, systematic study of these parameters influence was not carried out.

In addition, the feature of the research code is the possibility of calculating the phase equilibrium in the two approaches: a standard one is based on solving the problem of phase equilibrium in the hydrodynamic calculation, and the alternative approach, in which a decision is made in advance. Specifically, the parameters of phase equilibrium are approximated as a function of pressure and temperature and restored in the process of calculations [Belov et al], [Lysov et al], [Zhabkina and Myasnikov]. Currently this procedure is carried out to determine phase compositions, while the phase densities and viscosities are calculated from the known correlations. The latter approach has already been evaluated to be computationally inefficient [Lysov et al]. Finally, the accuracy of approximations depends on the polynomial degrees used. At the same time, the higher the degree of polynomials, the greater the amount of required computational operations to restore parameters of phase equilibrium. In the limiting case of zero degree approximation can be reduced to the standard approximation via K-values, which is the least accurate, but the most computationally efficient.

Thus, in light of the research code application to the problems of flow in high permeability reservoirs, there are some challenges: (1) to implement non-Darcy effects into research code; (2) to extend the functionalities of research code to simulate spatial flows, at least 2D; (3) to develop a research workflow, which for a specific problem and given accuracy make its possible to maximize the CPU efficiency by both increase of grid resolution and minimizing the approximation polynomials degrees. The developed workflow is then to be applied for modeling of some gas-condensate recovery optimization mechanisms.

## 1. Problem statement

Implemented into the research code, the system of equations describing two-phase multicomponent flow has the form :

$$\frac{\partial \phi b C_k}{\partial t} + \text{div} (U^l b^l C_k^l + U^g b^g C_k^g) + q_k = 0 \quad (1)$$

$$\frac{\partial \phi b}{\partial t} + \text{div} (U^l b^l + U^g b^g) + Q = 0 \quad (2)$$

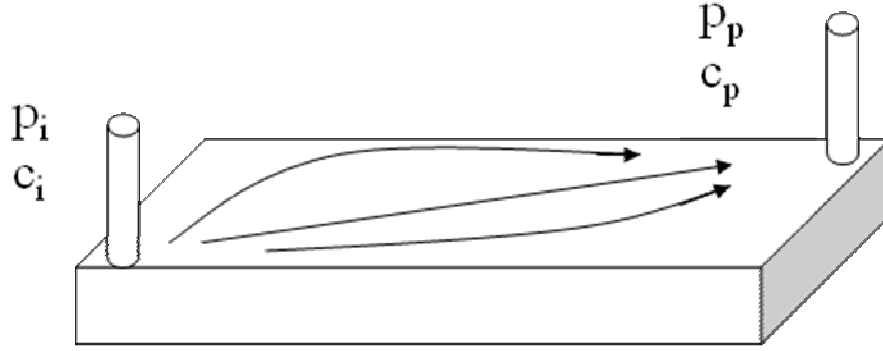


**Figure 1.** Schematic image of the computational domain. Indices  $i$  and  $p$  correspond to injector and producer. Depletion is modeled along the same scheme with specially chosen values of  $p_i$  and  $C_i$ .

where  $C_k$  - molar component concentration,  $b^{l,g}$  - molar phase densities,  $b = b^l S + b^g (1 - S)$ ,  $S$  - saturation,  $k = 1, \dots, N_C - 1$ . Source-terms  $q_k$  and  $Q$  describe inflow and outflow from a well and depending on boundary conditions may be evaluated with Peaceman formula or set to zero. In case when Darcy law is applicable and capillary effects are negligible we have:

$$U^{l,g} = -K(x, y) \frac{k^{l,g}(S)}{\mu^{l,g}(C)} \nabla P \quad (3)$$

Forchheimer equation is assumed to be traditional one for considering of inertial effects and in case of two-phase flow is given by:

$$-\nabla P = \frac{\mu^p(C)}{K(x, y)k^p(S)} U^p + \beta \rho^p U^p |U^p| \quad (4)$$

The review of non-Darcy models and empirical correlations of  $\beta$ -coefficient is to be found in [Melnikova and Myasnikov]. In the present work we use the correlation

$$\beta = \frac{4.8 \times 10^{10}}{K^{1.176}} \quad (5)$$

for debugging calculations and more complicated one for the problem of gas-condensate recovery optimization:

$$\beta = \frac{1.59 \times 10^3}{K^{0.5} \phi^{5.5}} \cdot \frac{1}{(1 - S_{wr})^{5.5} k_{rg}^{0.5}} \quad (6)$$

Equation (1)-(6) were solved in the domain of size  $L_x \times L_y \times 1$  in 2D and  $L_x \times 1 \times 1$  in 1D consequently, see Figure1. We used no-flow boundary conditions or cell with fixed pressure.

## 2. Computational Model

Hence it may be difficult to write the derivative of overall molar density  $\partial b / \partial t$  in (2) in general form, we treat it as a finite difference corrected during iterations on each time step. Its value at the first iteration is taken from the previous time step. Consider it is known at the  $n$ -th time step, as well as the primitive variables  $P, T, C$ , and phase compositions, densities and viscosities. Then, pressure distribution is obtained by implicitly obtained solution of the Poisson equation with non-Darcy effects. As for solution, we may choose either the method of alternating directions or the method of conjugate gradients. The algebraic multigrid algorithm is also planned to be implemented, but not yet. While method of conjugate gradients is considered to be more computationally efficient in comparison to alternating directions method in 2D problems, the latter is preferred in 1D cases. The concentrations are updated with newly obtained velocity field by explicit upwind scheme. The values of nonlinear coefficients in all equations are taken as an arithmetic average between first and current iterations. After the new values of concentrations, pressure and temperature are obtained, the phase equilibrium problem is solved either by calling for E300 flash procedure, or by restoring the data from the repository prepared at the preprocessing stage specially.

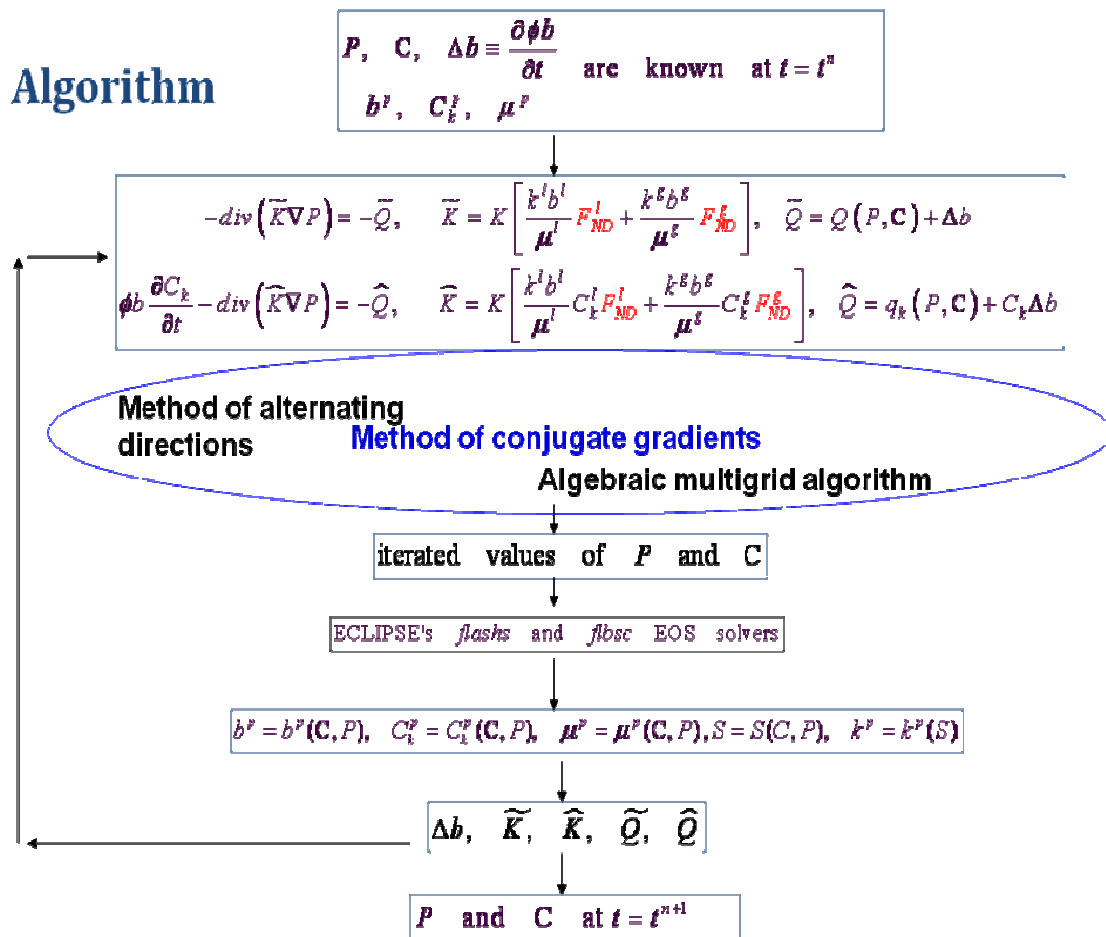


**Figure 2.** Main steps of algorithm implemented in the 1D and 2D compositional research code.

To implement Forchheimer equation, in other words, to define quantities  $F_{ND}^l$  and  $F_{ND}^g$  from Figure 2 we use the approach described in [Tavares et al]. Specifically from equation (4) we have:

$$U^p = -\nabla P \frac{Kk^p}{\mu^p} \frac{1}{1 + \frac{\beta\rho^p Kk^p}{\mu^p} |U^p|} \quad (7)$$

Let us put

$$F_{ND}^p = \frac{1}{1 + \frac{\beta\rho^p Kk^p}{\mu^p} |U^p|} \quad (8)$$

Then we obtain the Forchheimer equation, which differs from Darcy equation by additional factor  $F_{ND}^p$

$$U^p = -\nabla P \frac{Kk^p}{\mu^p} F_{ND}^p \quad (9)$$

Following equation (8) we have:

$$\frac{1}{F_{ND}^p} = 1 + \frac{\beta\rho^p Kk^p}{\mu^p} |U^p| \quad (10)$$

Substituting the expression inside the module with right part of (1.9) we obtain:

$$\frac{1}{F_{ND}^p} = 1 + \frac{\beta\rho^p Kk^p}{\mu^p} \left| -\nabla P \frac{Kk^p}{\mu^p} F_{ND}^p \right| = 1 + F_{ND}^p \frac{\beta\rho^p Kk^p}{\mu^p} \left| -\nabla P \frac{Kk^p}{\mu^p} \right| \quad (11)$$

Let us put

$$B = \frac{\beta\rho^p Kk^p}{\mu^p} \left| -\nabla P \frac{Kk^p}{\mu^p} \right| \quad (12)$$

where, for accuracy to be increased,  $\nabla P$  is taken from previous iteration, not from previous time step as it is done in [Tavares et al]. Finally, from (10) and (12), we obtain:

$$F_{ND}^p = \frac{-1 + \sqrt{1 + 4B}}{2B} \quad (13)$$

As it was already mentioned, the research code has been developed initially for making SLB for the development of new physical functionalities into Schlumberger streamline-based reservoir simulator (FrontSim). The idea there was to implement new effects into 1D research code which, being a stand alone code, solved the complete system of equations of course. However, only a part of it – namely composition transfer was initially planned to be implemented as an external subroutine into FrontSim as a along streamline 1D solver. The pressure solution in all streamline techniques is conventionally obtained from a separate 3D solution. However, it has been shown

that such approach lead to mistake in front position (Figure 3, upper figure, red lines). That is why it was decided that the complete system of governing equations should be solved along streamlines, in spite of the fact that the pressure is still determined from the 3D solution, and the 1D pressure is used only for more precise description of phase equilibrium. Results are presented at Figure 3 (upper part, red and blue lines and down-left part) Thus, the research code become the General purpose research code since in its 1D version it can be used for streamline simulations as an external solver along streamlines, but in 2D and 3D and, still in 1D version it can be used as a stand along research code.

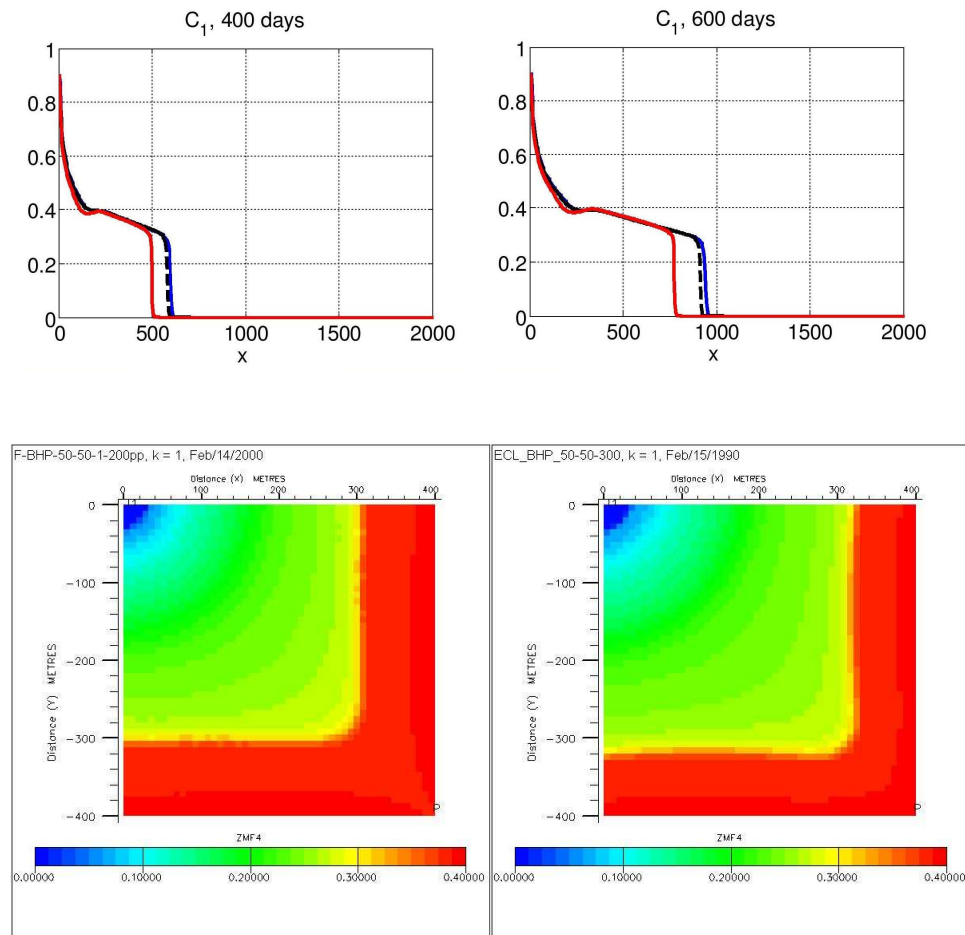


**Figure 3.** Comparison of E300 and RC/FrontSIM with and without updated pressure. Blue and black lines at upper panels correspond to E300 and RC+pressure update respectively. Red lines there – RS without pressure update. Left bottom panel is 2D E300 solution, right bottom panel – FS+pressure update.

### 3. Results of debugging calculations and grid optimization

To validate the 2D pressure solver and the total solution with Forchheimer equation, following numerical experiments were made. At first we studied the case with two wells: injector and producer, located at the corners of reservoir (Figure 1). Parameters of wells and reservoir may be found in Table1, Run #1.

**Table 1**

Run #	1	2	3
Mixture	C1 CO2 C4 C12	C1 CO2 C4 C10	C1 CO2 C4 C10
Composition in injector	(0.2, 0.78, 0.01, 0.01)	(0.2, 0.78,0.01, 0.01)	(0.2, 0.78, 0.01, 0.01)
Composition in reservoir	(0.23, 0.01, 0.3, 0.46)	(0.23, 0.01, 0.3 ,0.46)	(0.23, 0.01, 0.3, 0.46)
T, C	72	72	72°C
K, mD	200	100	100
P <sub>inj</sub> , bar	210	117	130
P <sub>prod</sub> , bar	30	113	100
Reservoir, X(m)xY(m)	2000 x 2000	2000 x 100	2000 x 100
Grid	MxN	Mx1	Mx1
Injector coordinates	(1,1)	(1,1)	(1,1)
Producer coordinates	(M, N)	(M, 1)	(M, 1)

To demonstrate strong non-Darcy effect influence the model correlation (5) was used with  $\beta$ -coefficient was three time as higher as that calculated one, specifically  $\beta \approx 3 \times 10^8 \text{ cm}^{-1}$ . Figure 4 shows the concentration distribution of the first component of the same points in time, resulting from calculations on the E300 (left panels) and the research code (right panels) in the case of Darcy flow (top) and Forchheimer flow (bottom). With good match for all the results one can observe some boundary effects. These effects are well known in reservoir simulation community and people believe they can overcome the problem by implementing 9-point scheme instead of 5-point one (which is used to obtain both solutions here). However, the simulation results of the same flow with 9-point scheme implemented into E300 have shown that the problem is something else. Indeed, Figure 5 shows that boundary effects disappeared on a 120x120 grid if a 9-point scheme is applied in the E300 simulations, but appeared again on a finer grid. Since the study of the peculiarities of 2D and 3D pressure solution is not the major goal of this research we just point out the problem here and go further with our validating with 1D models.

Let us verify the order of approximation of the schemes implemented in E300 and research code. For this we construct a shock-free solution in the one-dimensional displacement problem, for

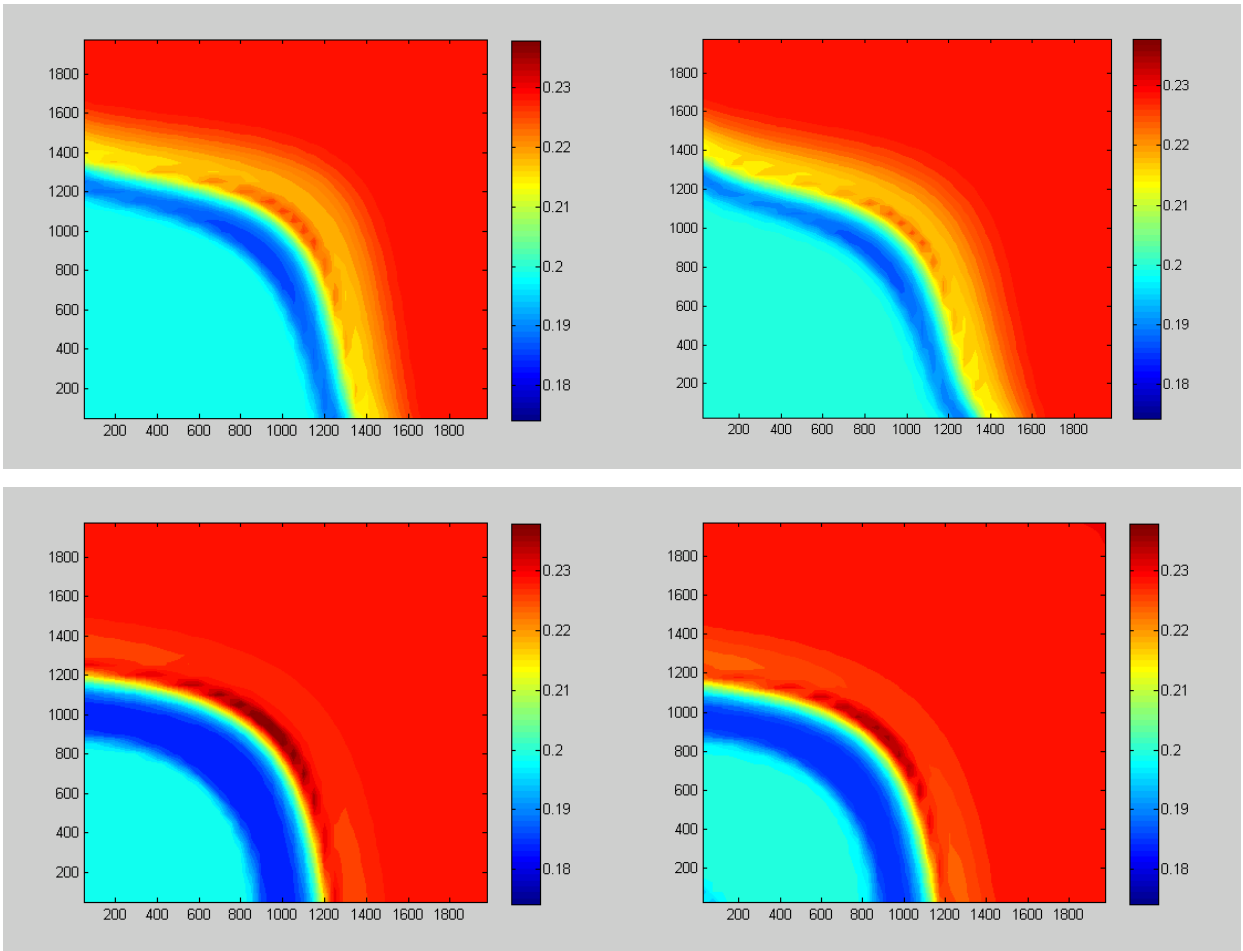


**Figure 4.** Concentration distribution of the first component of the same points in time, resulting from calculations on the E300 (left panels) and the research code (right panels) in the case of Darcy flow (top) and Forchheimer flow (bottom)

which we took the compositions in the reservoir and the injector sitting inside the two phase domain on one and the same node at reservoir pressure and temperature conditions and then vary pressure slightly during the simulations to avoid shock appearance due to pressure change (Run #2 in Table 1). The results of calculations performed with E300 and the research code on a system of several grids with dimension factor of three are presented in Figure 6. Trebling points in the finite-volume sampling made it possible to obtain a set of points belonging to each of the grids. Then in the obtained sets of points the relative error from the reference solution was calculated. In our case we assume 3240 cells solution to be reference. The results of these experiments show that the relative error in  $L_2$  norm decreases almost by 3 times with increasing dimension of the grid in the same 3-fold, thus the two schemes are of first-order approximation.

We now consider the shock-type displacement, (Run #3 in Table 1). Figure 7 shows the convergence of E300 to the reference solution of 87480 cells (bold red line). Just as in the shock-free case, the dimension of the grid increases by a factor 3, but the norms ratio is less than 3 (see table 2) and tends to 3 with increasing the dimension of the grid.

To answer the question with which speed the solution tends to convergence, let us return to Figure 7, where a bold green line denotes the solution obtained by a research code on the grid with 360 cells. The difference from the reference solution is 5.5%, while the E300 on the same grid differs by 10.2% (see table 3).

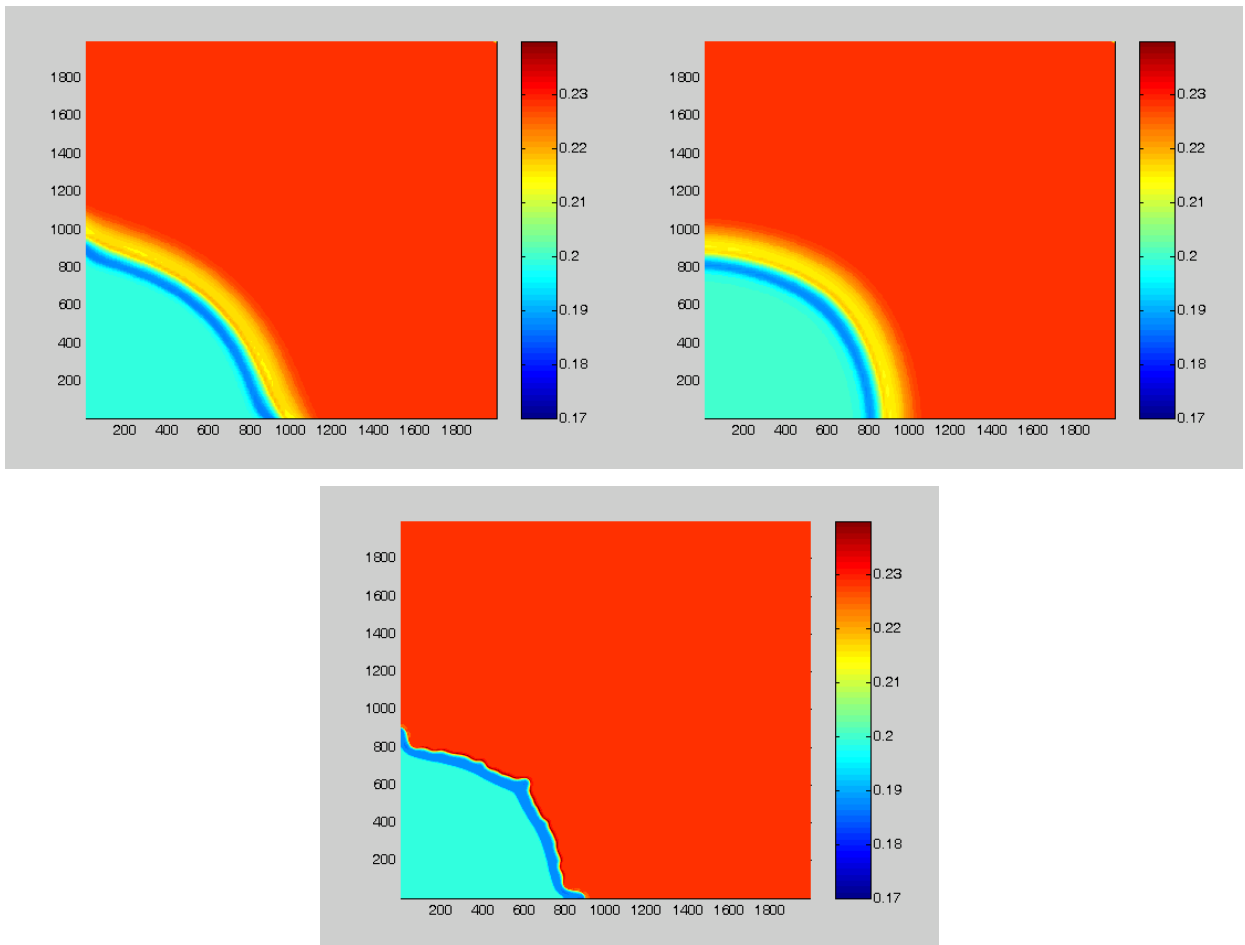


**Figure 5.** Results of displacement problem simulation with different calculations schemes. Top left panel – E300, 120x120, 5-point scheme; Top right panel – E300, 120x120, 9-point scheme; Bottom panel – E300, 1080x1080, 9-point scheme.

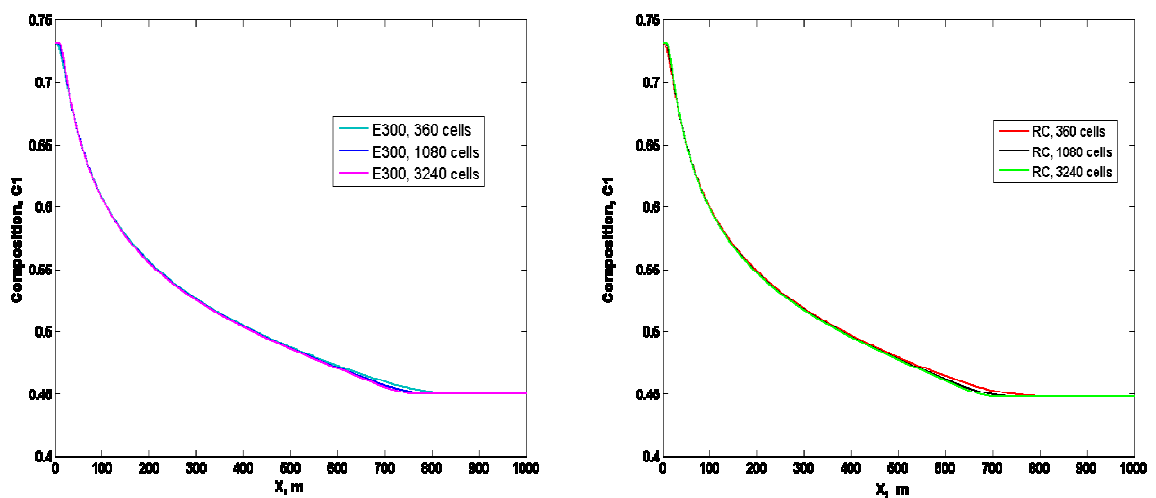


**Figure 6.** Calculations of free-shock displacement, performed with E300 (left panel) and RC (right panel)

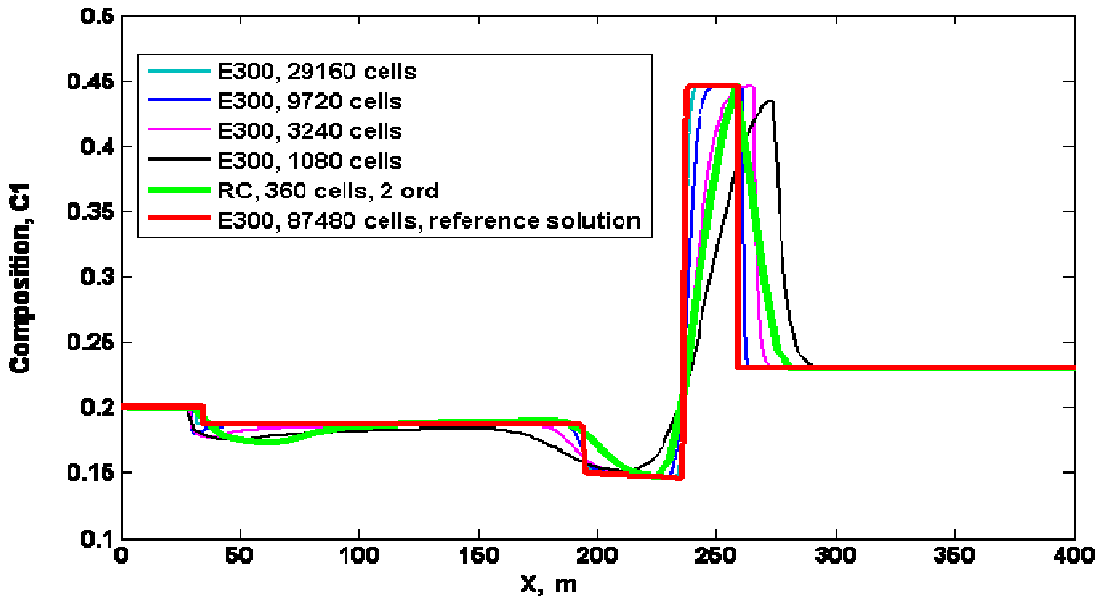


Figure 7. Shock solution (E300, all lines except bold green) and RC (bold green line)

Table 2

Solution	Norms L2 E300, 87480 cells – reference solution	Grid resolution	ratio	Norms L2 ratio
E300,1080 cells	7.9%	3	3	1.52
E300, 3240 cells	5.2%			
E300, 9720 cells	3.0%			
E300, 29160 cells	1.4%			
				1.73
			3	2.14

Table 3

Solution	Norms L2 E300, 87480 cells – reference solution
RC, 360 cells	5.5%
E300, 3240 cells	5.2%
E300, 360 cells	10.2 %

The reason is that so called higher resolution scheme is implemented in the research code as an option. Such schemes are well known in computational hydrodynamics and become popular now in reservoir simulation community [Malison et al]. Specifically to the system (1)-(6), the question on the scheme resolution is related to how one calculate functions  $f_{i+1/2} = \tilde{K}, \hat{K}$  (Figure 2), defined on the intercell boundaries. We need to know there phase densities, relative permeabilities and phase viscosities which all are functions of composition determined at the center of the cell. One can use (as it was used before) the simplest first order accuracy upwind specification for all the listed functions:  $f_{i+1/2} = f_i$  if  $P_{i+1} - P_i < 0$ , and  $f_{i+1/2} = f_{i+1}$  otherwise. The higher resolution scheme can be constructed if one defines

$$f_{i+1/2} = X_i + \frac{1}{4} \left\{ (1+\eta) \tilde{\Delta}_{i+1/2} + (1-\eta) \tilde{\tilde{\Delta}}_{i+1/2} \right\} \quad (14)$$

where

$$\tilde{\Delta}_{i+1/2} = \min \text{ mod } \{ \beta \Delta_{i-1/2}, \Delta_{i+1/2} \}, \quad \tilde{\tilde{\Delta}}_{i+1/2} = \min \text{ mod } \{ \Delta_{i-1/2}, \beta \Delta_{i+1/2} \} \quad (15)$$

$$-1 \leq \eta < 1, \quad \beta \leq \frac{3-\eta}{1-\eta}, \quad \min \text{ mod } \{ x, \beta y \} = \text{sgn}(x) \max \{ 0, \min[|x|, \beta y \text{sgn}(x)] \}, \quad (16)$$

The values  $X_i$ ,  $\Delta_{i+1/2}$  can be optionally defines as  $X_i = f_i$ ,  $\Delta_{i+1/2} = f_{i+1} - f_i$ , or, to attain “second” order approximation in space and in time, as  $X_i = f_i^*$ ,  $\Delta_{i+1/2} = f_{i+1}^* - f_i^*$ , where asterisk denotes the values obtained as a result of a half-time promotion of the solution by the first order accuracy scheme (“predictor-corrector” technique). With the maximal values of compression parameters  $\beta$  this technique allows to increase the resolution properties of the scheme in 9 times (the solution presented by bold green curve in Figure 7 was obtained with  $\eta = 0.5$ ).

#### 4. The optimization results of hydrodynamic calculations based on phase equilibrium approximations

The approximative technique being developed in SMR for several years is based on the physical fact that in thermodynamic equilibrium there is one-to-one correspondence between bubble points and dew points within a two phase domain. That means, that tie lines (segment across the two phase domain) do not intersect inside it and one can introduce alternative set of independent variables. Namely, for the fixed pressure and temperature each point inside a two phase domain of phase space can be characterized by a scalar ‘leading component concentration’  $C_1$  and a vector-parameter of tie-lines and  $\gamma = \{C_2^m, \dots, C_{N_c-1}^m\}$ . The change of the variables from the set  $C_1, C_2, \dots, C_{N_c-1}$  to the set  $C_1, \gamma$  has a series of advantages; one of them is that the new set variable is very convenient to perform the precise approximation of phase equilibrium.

In the developed in [Belov et al] approximation, so called Q-values

$$Q_k(\gamma) = \frac{C_L^k - C_G^k}{C_L^k + C_G^k} = \frac{1 - K^k}{1 + K^k} \quad (17)$$

are primarily approximated by polynomials in the transcendental way:

$$Q_1^2 = P_1(\vec{\gamma}), \quad Q_k = Q_1 P_k(\vec{\gamma}) \quad (18)$$

The degrees of polynomials can be arbitrary, the higher they are the more precise the approximation is and the more CPU time is expected to reconstruct the phase parameters during hydrodynamic simulations. The simplest case of zero degrees is equivalent to the constant  $K$ -values case. Originally, the polynomial approximations were constructed for the fixed  $P$  and  $T$ . If one need to perform the hydro simulations for the known range of pressure and temperature variations he has to perform the preprocessing work of approximation construction for each  $P$

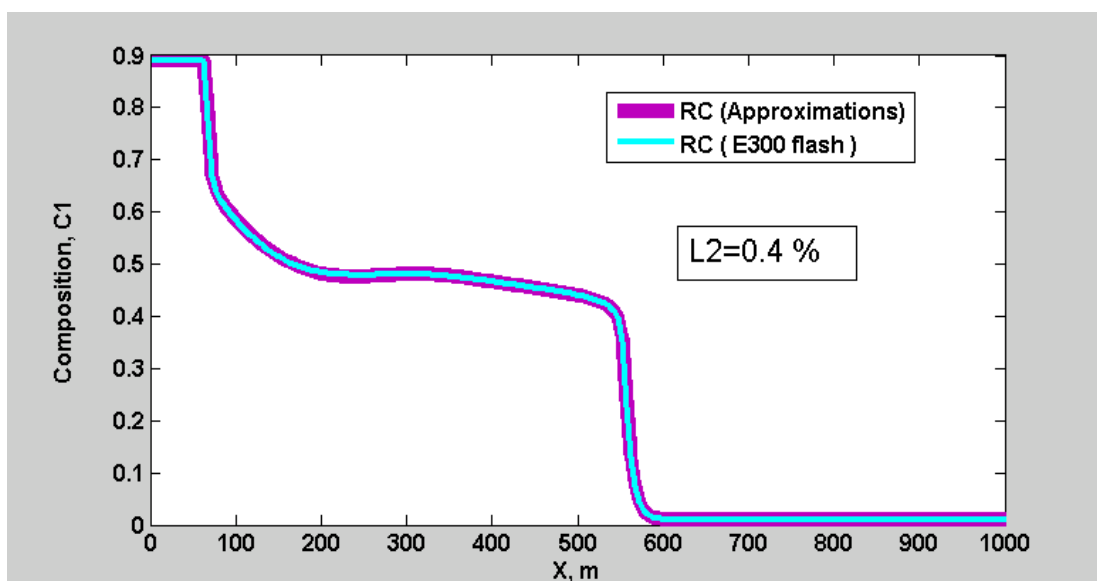


**Figure 8.** Comparison of two options implemented into RC: E300 flash and approximations

and  $T$  in the range, put the polynomial coefficient in a storage and understand a rule how to take them off there during the simulation. While in the previous methodology approximation of phase viscosities and densities was carried out and even recommendations for optimal selection of polynomials degrees were made, in the hydrodynamic calculations the known correlations of these quantities were used, that appeared to be computationally inefficient.

In the present work we extended the approximations on viscosity and density, having in mind, however, that they depend on composition in one phase domain and the approximations are not applicable there.

Figure 8 shows comparison of two options implemented into Research code: E300 Flash and approximations for a three component C1C4C6 mixture with all polynomial degrees equal to 2 and with pressure range splitting in 20 parts. As one may see, approximations give perfect coincidence: these cases differ by only 0.4% in L2 norm.

Below is a schedule of CPU cost in case of E300 Flash and approximations (Figure 9). It is seen that the gain in the case of approximations is 3 times. The benefits of using approximations of densities and viscosities are not very noticeable, as in one-phase region E300 Flash was used.

Together with the result of the previous section, the purpose of the use of phase equilibrium approximations can be formulated as follows. For the given problem, given mixture and given flow regimes (pressure rates, NonDarcy parameters etc) to tune the problem in the simplified regimes by minimizing the required grid, and the polynomial degrees which still provide the desired accuracy. The accuracy here is external parameter and, for researcher, can be either fixed or changed during the research process. That tuning can be performed on 1D problem and then used for 3D, or, for steady state problem and then used for transient one. While the proposed workflow is not automatic, it could be very valuable for solving time consuming research problems such as ones related to gas-condensate flows problems in well-bore zones and naturally-fractured reservoirs.

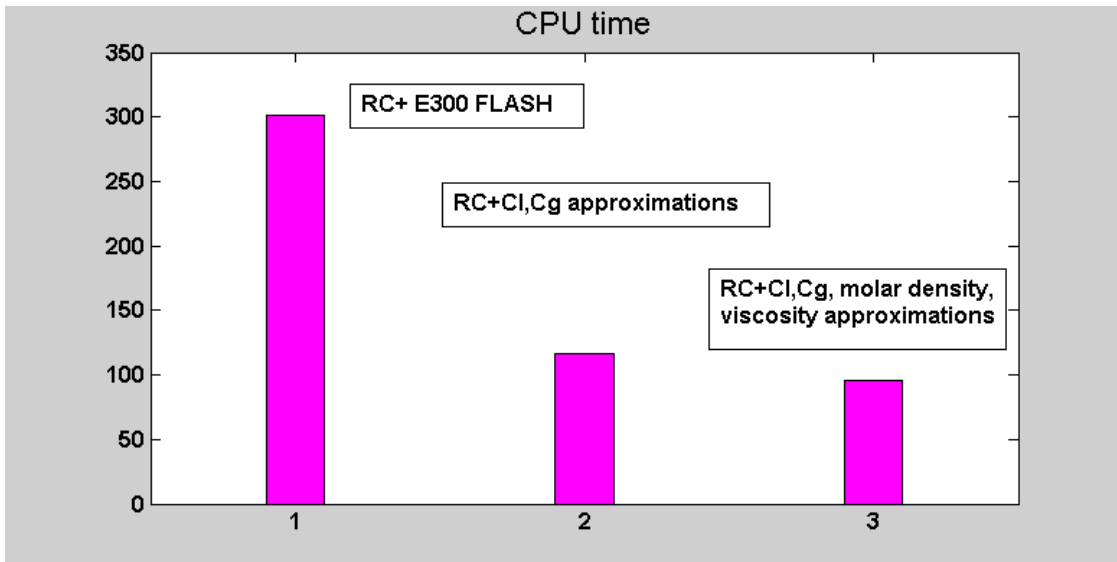


Figure 9. Comparison of time-consuming in case of E300 flash and approximations.

## 5. Comparison of two optimizations

The previous sections have described two approaches to significantly improve the efficiency of the research code. First, it is reducing the size of the computational grid, and secondly reducing the time cost by minimizing the reconstruction parameters of phase equilibrium in the hydrodynamic calculation. Figure 10 shows the result of combining these two approaches. It is easy to see that in the result of the use of approximations, the accuracy is not only not diminished, but even increased and amounts to 4.7%

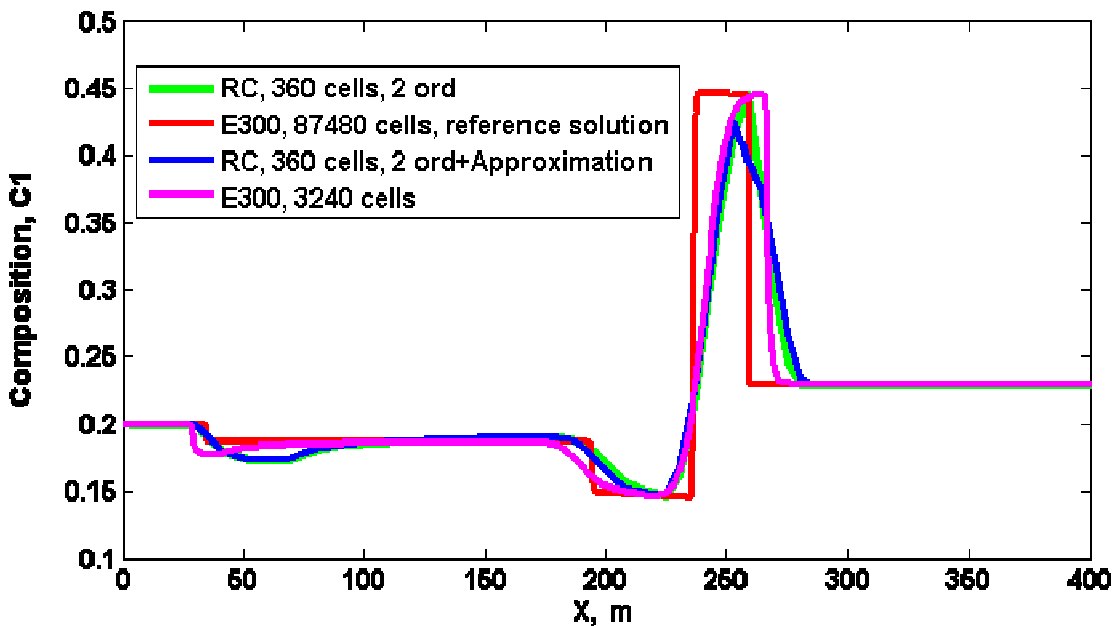
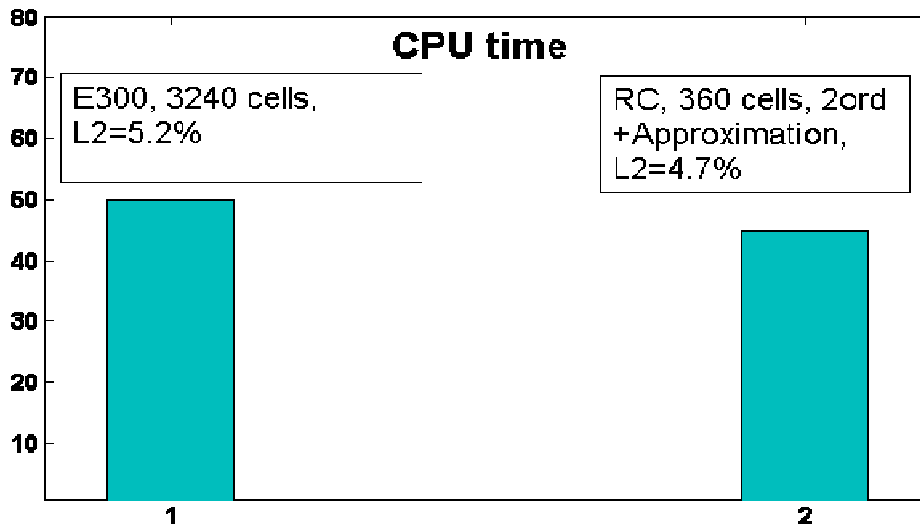


Figure 10. Comparison of optimization methods efficiency



**Figure 11** Time-consuming chart for E300 and RC.

But of particular interest is the timing diagram. It can be seen that to achieve the same accuracy of the solution time costs of our research code is comparable or even less than the cost of commercial simulator E300. Although E300 has a clear CPU advantage with respect to the RC in the sense of relative to the cell numbers CPU time, the result in Figure 11 can be considered as an achievement. The point is that E300 is an optimized (in a programming sense) commercial simulator with very good time stepping algorithm, while RC is a not optimized, and chose of a time step is made by the simplest CFL condition. However, Figure 11 indicates that we can use the RC with the same absolute efficiency as E300 for the research purposes where E300 is not convenient for applications for some reasons.

## 6. Application: Optimization of gas-condensate recovery

As practical application of this research we consider the problem about optimization of gas-condensate recovery. During the development of gas condensate fields pressure can significantly reduce and become lower than the dew point. This leads to the phenomenon of retrograde condensation when gas in the isothermal case turns into liquid because of pressure decreasing. Formed condensate creates the so-called condensate-bank preventing from gas movement. Even when oil saturation reaches its critical value, oil mobility is still much less than gas mobility, that adversely affect the production of gas. Therefore, the question of interest is to find technological regime, allowing to decrease the size of bank conserving gas production.

At the beginning of the study two cases with two horizontal wells located in the high-permeability zone were considered, see Figure 12. We considered the 9-component mixture with composition N2 C1 C2 C3 IC4 NC4 F1 F2 F3 identified as a simplified realistic composition of Vuktylskoe Field.

In the first case the size of the area with constant inflow was small enough to create a non-standard condensate structure. Namely, at first condensation occurred exactly in the area of equipotential surface  $P = P_{dew}$  (boundary of dark blue colored zone in left panels of Figure 13), forming U-shaped structure just above the high-permeability zone.

Accumulated enough, condensate broke down under the force of gravity, accumulated in the bottom of high-permeability zone, and began to flow steady in the production well located

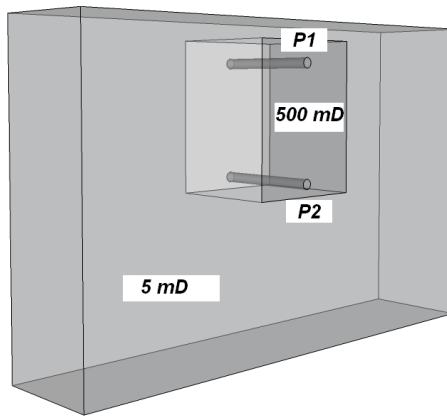


**Figure 12.** Scheme of gas-condensate flow simulated with E300.

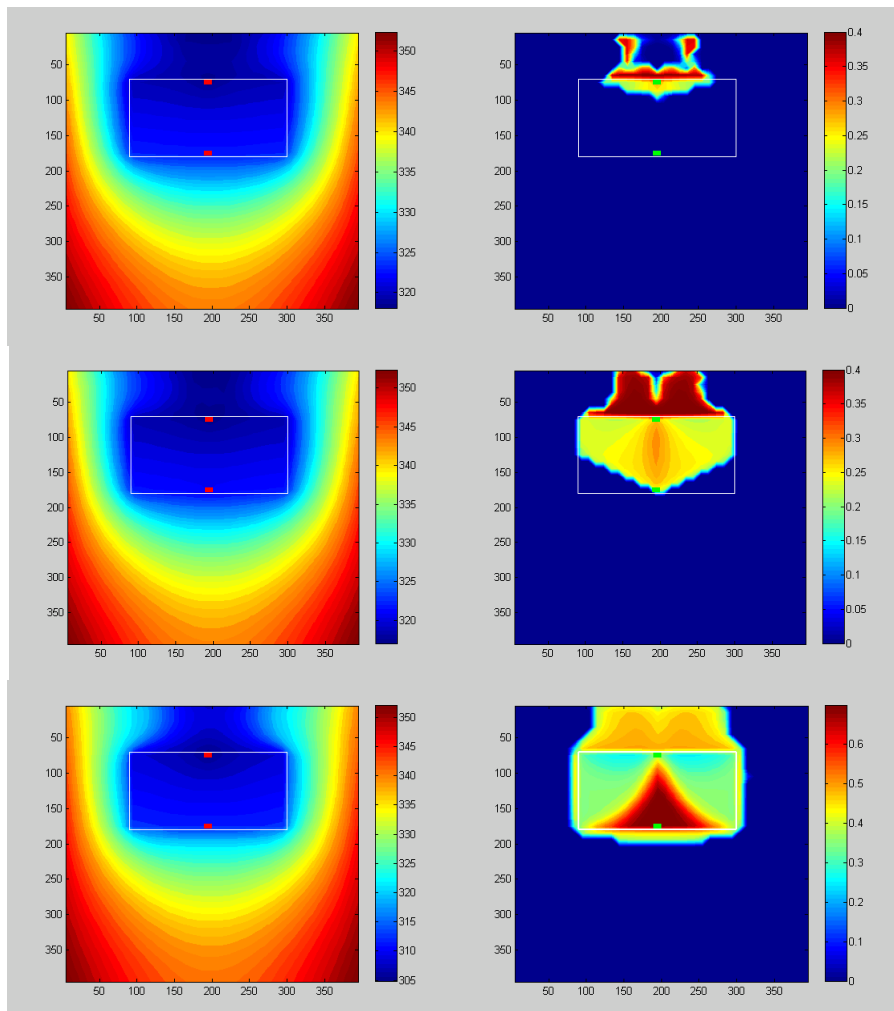


**Figure 13.** Pressure(left) and saturation distributions (right) at different moment of for regime presented in Figure 12

below. However, it seems that the oil recovery at a fixed gas production does not change depending on whether we use one well or two, as described above. This is due to the large volume of produced gas and small fraction of produced condensate compared to condensed gas at the surface.

The next experiment was done to minimize the total flow rate with hope to see a greater contribution of condensate field in the resulting output. For this the computational domain was expanded, and that resulted in accumulating of the entire condensate not the on the top of high-permeability zone, but at lateral part of it. The simulations with different well(s) positions inside the high permeable zone indicated that in terms of gas / condensate recovery in this regime, the best scenario was for one well located at the bottom of the permeable zone, as could be expected beforehand.

Therefore, we then decided to look for further solution in a class of time-dependent impacts on condensate banks. Following [Rudenko & Kuzmichev], it was suggested to restore the pressure up to initial reservoir value by varying the bottom hole pressure in bottom wells (Figure 14), and, consequently, to reduce the mass of condensate. But, ultimately, as a result of such stimulation, cumulative production of oil and gas declined. Since at that time we already knew that the result of periodical BHP change could depends on the frequency of that change [Zhabkina & Myasnikov], and, at the same time it was technically quite inconvenient to introduce periodic change of boundary conditions in E300 data file, we decided to pass the same mixture through the similar exercise as was done in [Zhabkina & Myasnikov] for the 3 component model mixture.

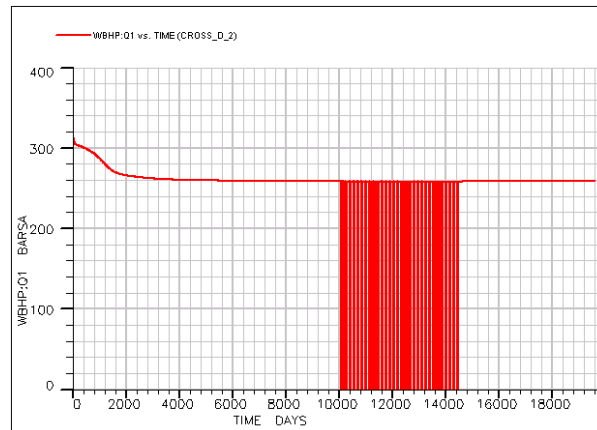


**Figure 14.** BHP pressure over time

Namely, we considered one dimensional flow in  $X \times Y \times Z = 400 \times 1 \times 1 \text{ m}^3$  reservoir with uniform permeability  $K = 100mD$  and porosity  $\phi = 0.13$ , where one producing well is placed in the first grid cell. Pressure, composition and temperature are kept fixed constant at the outer boundary and chosen such to provide a mixture to be in a gas phase there. At the hole, pressure is considered to a certain function of time, in particular, constant:

$$P(t) = \begin{cases} P_w(1 + A \sin^\alpha(\omega(t - t_0))), & t > t_0, \\ P_w, & t \leq t_0 \end{cases}, \quad A = \frac{(P_{res} - P_w)}{2P_w}, \quad \alpha = 1, 2 \quad (19)$$

For the initial temperature, and the expected during depletion pressure, mixture is below dew point at the hole.

The developed above optimizing technique was applied when we studied this flow. Specifically, we considered at first the case with constant value of borehole pressure ( $t_0 = \infty$  in (19)) where the flow solution for a given stationary boundary conditions after a certain time after the start of depletion reaches a steady-state (Figure 15). We found out then that simulations performed on 50 grid point with the high resolution scheme with  $\eta = 0.5$  and maximum compression provide acceptable accuracy with the minimal CPU time for both steady-state and transient regimes (Figure 16).

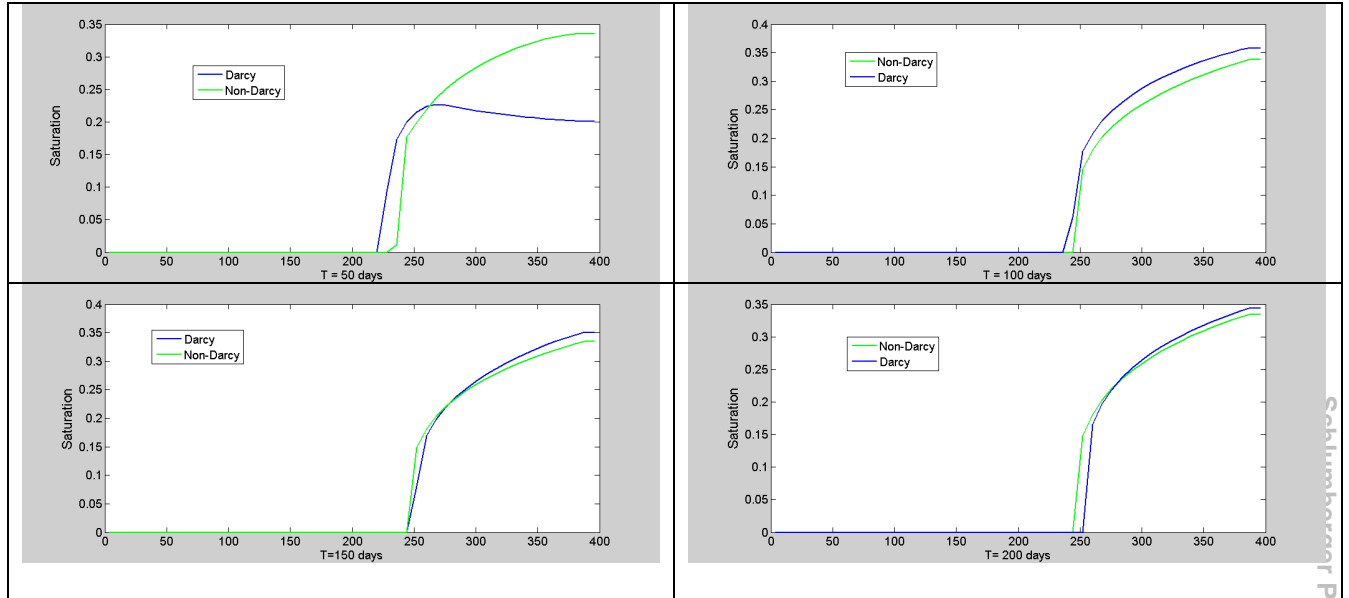


**Figure 15.** Steady- state gas condensate bank in case of Darcy and Forchheimer models for depletion test-problem. The solutions are obtained by the 1<sup>st</sup> order scheme on 50 cells).

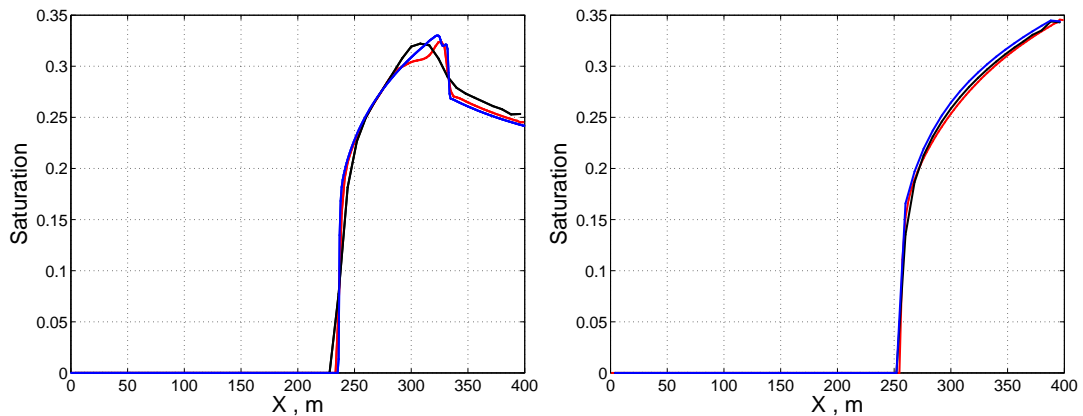


**Figure 16.** RC solution obtained with higher resolution scheme reaching the stationary state ( $t = 70$  and  $t = 200$  days). Black, red, blue lines stand for grid with 50, 150, 450 cells.

Optimization in terms of approximating polynomial degrees has not been performed in this case because of the fact that the concentration of heavy elements in the gas phase is small. The thing is that one had to choose the high degree of polynomials to ensure the positivity of these quantities and, therefore, the approximation becomes time-consuming. Additional research

addressing such cases should be held in the future (to consider the possibility to simply null these values if they become negative, for example).

As a result of simulations with  $t_0 = 260$  in (19), cumulative condensate mass excess was obtained over time, see Figure 17. In contrast to [Zhabkina & Myasnikov], for real formation mixture we found no positive effect when  $\alpha = 1$ . Nevertheless all the results are understandable from a physical point of view. Additional studies of influence of mixture composition as wells as non-stationary regimes are of undoubted interest.

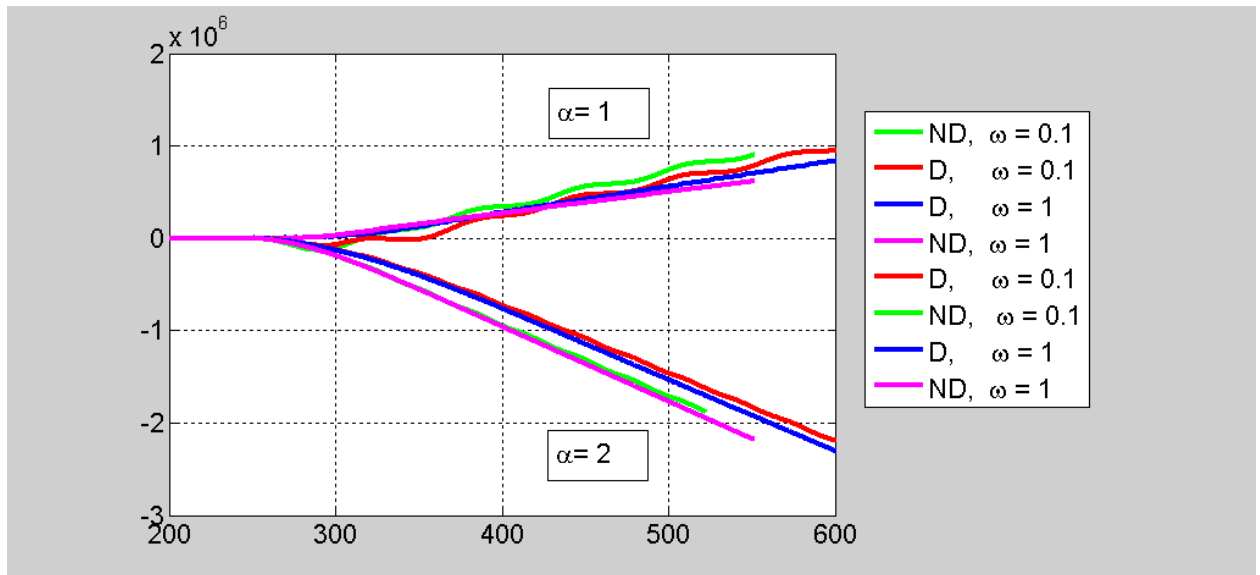


**Figure 17.** RC solution (total cumulative excess of condensate in the reservoir), obtained with higher resolution scheme in the process of perturbation of the stationary condensate banks in different modes.

## Conclusion

In the present study the following results were obtained:

A “General Purpose” Research code for fast/precise solution of non-Darcy multicomponent two-phase non-isothermal flow with phase transitions has been developed and validated against E300. Having a higher resolution and preprocessing approximation of phase diagram as options, the code provides the desired accuracy in less CPU time as conventional ones. In particular, it demonstrated good coincidence with E300 in accuracy and time consuming.

A workflow that minimize the grid size and polynomial degrees requested for a specific problem solution with a desired is suggested and primarily validated. Such minimization may lead to significant decrease of CPU time which is important for heavy simulations.

An attempt to apply the suggested workflow to optimize condensate recovery in gas-condensate reservoirs with high permeable zones is undertaken. The experiments with E300 simulation demonstrated the necessity of non-stationary BHP effect modeling. Dependences of the condensate mass change of at different vibrational modes with and without non-Darcy effects were obtained. There are both positive and negative effects.

## References

[Belhaj et al]:

H.A. Belhaj, K.R. Agha, S.D. Butt, M.R. Islam, Dalhousie University: “Simulation of Non-Darcy Flow in Porous Media Including Viscous, Inertial, and Frictional Effects”, SPE 84879 (October 2003), 7 p.

[Belov et al]:

Belov N., A. Myasnikov, K. Bratvedt, “Precise Approximations of Phase Equilibrium of Multicomponent Hydrocarbon Mixtures”, OFSR/RN/2008/068/SMRMM/C

[Levkovich et al]:

Levkovich-Masluk L., V. Lysov, Yu. Rykov, A. Myasnikov, K. Bratvedt, “Fast Compositional Solver in Streamline-Based Reservoir Simulations: Constant K-value Approximations”, OFSR/RN/2008/070/SMRMM/C

[Lysov et al]:

Lysov V., O. Podgornova, Yu. Rykov, A. Myasnikov, K. Bratvedt, “Fast Approximation of Phase Equilibrium Based on Random Sampling and its Application for Compositional Streamline Simulations”, OFSR/RN/2008/071/SMRMM/C

[Malison et al]:

B.T. Mallison, M.G. Gerritsen, K. Jessen, and F.M. Orr Jr., SPE, Stanford U.: “High-Order Upwind Schemes for Two-Phase, Multicomponent Flow”, SPEJ 10.3 (September 2005), 15 p.

[Mohan et al]:

Mohan, J., Pope, G.A. And Sharma, M.M.: “Effect of Non-Darcy Flow on Well Productivity of a Hydraulically Fractured Gas-Condensate Well”, SPE Reservoir Evaluation & Engineering (August 2009), 10 p.

[Rudenko & Kuzmichev]:

Rudenko D., Kuzmichev D., 2010, Private Communication

[Tavares et al]:

Carlos Alberto Pereira Tavares, SPE, Questa Engineering Corp., and Hossein Kazemi, SPE, and Erdal Ozkan, SPE, Colorado School of Mines: “Combined Effect of Non-Darcy Flow and Formation Damage on Gas-Well Performance of Dual-Porosity and Dual-Permeability Reservoirs”, SPEJ 9.5 (October 2006), 10 p.

[Zhabkina & Myasnikov]:

Zhabkina A., Myasnikov A., “Modeling of multicomponent non-isothermal filtration in a near-wellbore zone”, 2010, OFSR Department Note, submitted

[Melnikova and Myasnikov]:

Melnikova Yu., Myasnikov A., “A Review of non-Darcy models and Empirical Correlations of beta-coefficient”, 2010, OFSR Department Note, in preparation

[Mohan et al]:

Mohan, J., Pope, G.A. And Sharma, M.M.: “Effect of Non-Darcy Flow on Well Productivity of a Hydraulically Fractured Gas-Condensate Well”, SPE Reservoir Evaluation & Engineering (August 2009), 10 p.